Human Molecular Genetics, 2011, Vol. 20, No. 16 **3198–3206**
doi:10.1093/hmg/ddr225
Advance Access published on May 19, 2011

Conditional deletion of Ccm2 causes hemorrhage in the adult brain: a mouse model of human cerebral cavernous malformations

Kirk Cunningham[1,†], Yutaka Uchida[2,†], Erin O'Donnell[2,†], Estefania Claudio[1,†], Wenling Li[2], Kosha Soneji[2], Hongshan Wang[1], Yoh-suke Mukouyama[2,*] and Ulrich Siebenlist[1,*]

[1]Immune Activation Section, Laboratory of Immunoregulation,National Institute of Allergy and Infectious Diseases and [2]Laboratory of Stem Cell and Neuro-Vascular Biology, Genetics and Developmental Biology Center, National Heart, Lung, and Blood Institute, National Institutes of Health, Bethesda, MD 20892, USA

Received February 27, 2011; Revised and Accepted May 16, 2011

Cerebral cavernous malformations (CCM) are irregularly shaped and enlarged capillaries in the brain that are prone to hemorrhage, resulting in headaches, seizures, strokes and even death in patients. The disease affects up to 0.5% of the population and the inherited form has been linked to mutations in one of three genetic loci, *CCM1, CCM2* and *CCM3*. To understand the pathophysiology underlying the vascular lesions in CCM, it is critical to develop a reproducible mouse genetic model of this disease. Here, we report that limited conditional ablation of *Ccm2* in young adult mice induces observable neurological dysfunction and reproducibly results in brain hemorrhages whose appearance is highly reminiscent of the lesions observed in human CCM patients. We first demonstrate that conventional or endothelial-specific deletion of *Ccm2* leads to fatal cardiovascular defects during embryogenesis, including insufficient vascular lumen formation as well as defective arteriogenesis and heart malformation. These findings confirm and extend prior studies. We then demonstrate that the inducible deletion of *Ccm2* in adult mice recapitulates the CCM-like brain lesions in humans; the lesions display disrupted vascular lumens, enlarged capillary cavities, loss of proper neuro-vascular associations and an inflammatory reaction. The CCM lesions also exhibit damaged neuronal architecture, the likely cause of neurologic defects, such as ataxia and seizure. These mice represent the first CCM2 animal model for CCM and should provide the means to elucidate disease mechanisms and evaluate therapeutic strategies for human CCM.

INTRODUCTION

Cerebral cavernous malformations (CCM) are vascular lesions that occur most commonly in the central nervous system of patients (reviewed in 1,2). The lesions are prone to hemorrhage; they are histologically characterized by thin-walled, enlarged capillary cavities, lacking smooth muscle support. Symptoms in patients range from severe headaches to seizures, neurologic disorders and ultimately strokes that can lead to death. CCM lesions are detected at a frequency of 1 in 200–250 individuals in the general population and they occur in a sporadic or in a familial form. The familial form is inherited in an autosomal dominant fashion with incomplete penetrance (1). The disease is associated with inherited loss-of-function mutations in one allele of three distinct genes, *CCM1* [*KRIT1* (*KREV1/RAP1A interaction trapped-1*)], *CCM2* [*OSM* (*Osmosensing scaffold for MEKK3*)*; Malcavernin; MCG4607*] or *CCM3* [*PDCD10* (*Programmed cell death 10*)] (1,2). Many germline mutations have been identified, and with few exceptions, they appear to severely cripple or fully inactivate the expression of the encoded protein. In recent years, evidence has mounted implicating a somatic loss of the second allele as the ultimate cause of the disease. Although technologically challenging, careful

*To whom correspondence may be addressed at: NIH, Bldg. 10, Rm. 6C103, Bethesda, MD 20892, USA. Email: mukoyamay@mail.nih.gov (Y.-s.M.); NIH, Bldg. 10, Rm. 11B15A, Bethesda, MD 20892, USA. Email: ulrich.siebenlist@nih.gov (U.S.)
†The authors wish it to be known that, in their opinion, the first four authors should be regarded as joint First Authors.

analyses of lesions have uncovered second mutations in the allele opposite the inherited one in lesions, which would completely eliminate expression of a functional CCM protein from both alleles of the affected locus, at least in a portion of the cells within a given lesion (3–6).

Critical insight into the *in vivo* functions of CCM proteins was gained from mouse models genetically engineered to lack expression of CCM proteins (1). Loss of either *Ccm1* (7), *Ccm2* (8–10) or, most recently, *Ccm3* (11) resulted in embryonic lethality, associated with grossly defective angiogenesis. The targeted null mutations in *Ccm* genes caused growth arrest after E8.5 and the embryos were generally dead by E10–11. Growth arrest was accompanied by defects in angiogenic remodeling in the peripheral vasculature and lumen formation in the branchial arch artery connecting the heart with the dorsal aorta, thus apparently constricting blood flow and resulting in failure to fully establish circulation. These data seem to suggest that CCMs are required for proper angiogenesis; however, the potential requirement for blood flow in angiogenesis makes it difficult to distinguish a primary requirement of CCM proteins in angiogenesis from a secondary defect due to abnormal heart development and function. Furthermore, the early embryonic lethality in mice with homozygous knockout of *Ccm* genes precludes studies of the role of CCM in the cerebral vasculature.

Whether human CCM lesions are caused by loss of *CCM* genes in vascular cells or neuronal cells has been a matter of debate (12,13). More recently, conditional loss of *Ccm* genes in vascular endothelial cells (ECs), smooth muscle cells (SMCs) and/or neuronal cells in mice has been accomplished (8–11). Deletion of floxed *Ccm2* or *Ccm3* in ECs using a *Tie2-Cre* driver caused cardiovascular defects, resembling the phenotypes seen in conventional knockout of *Ccm2* or *Ccm3*, whereas loss of *Ccm2* or *Ccm3* in neuronal cells using a *Nestin-Cre* driver or loss of *Ccm3* in SMCs using a *SM22α-Cre* driver failed to replicate such phenotypes. These findings do indicate that expression of CCM proteins in ECs is required for proper cardiovascular development, although a very recent study suggests that loss of *Ccm3* in at least some neuroglial cells may also have a role in forming proper vascular structures (14). Several additional lines of evidence have suggested roles for CCM proteins in cellular processes of particular relevance to endothelial cell functions. A prior ultra-structural analysis of excised CCM lesions from patients noted deficient tight junctions between adjacent ECs (15). In addition, biochemical approaches have implicated CCM proteins in cell adherence and tight junction formation, cell polarity, cell–matrix adhesions and cytoskeletal architecture (this has been extensively reviewed by 16); specifically, CCM proteins have been physically and functionally linked to several cell surface receptors present on ECs, such as cadherins, integrins, HEG1 and VEGFR2, as well as to several intracellular regulators that have roles in the aforementioned processes, such as ICAP1, Rap1, Rho family GTPases and MEKK3/p38. These findings support the notion that CCM proteins play central roles in endothelial cell–cell interactions required for proper lumen formation and for maintenance of the vascular barrier.

Despite considerable efforts, a useful mouse model for the human diseases does not exist. Mice with heterozygous loss of *Ccm1* or *Ccm2* do not develop lesions with any useful frequencies, even when mice were further engineered to favor increased mutational rates, a context which itself may seriously compromise results (2,17). Here, we first analyzed conventional and endothelial-specific knockouts of *Ccm2*, confirming and extending prior reports that implicated endothelial cell-specific loss of CCM2 function in cardiovascular development. We then generated a mouse model that appears to faithfully recapitulate the human CCM lesions; in this model, we induced limited conditional deletions of *Ccm2* in blood-accessible cells and ECs of young adult mice; some of these mice were observed while exhibiting neurological dysfunctions, including ataxia, and all had developed brain hemorrhages resulting from cavernous malformations, ultimately resulting in the death of animals over time.

RESULTS

Generation of *Ccm2* mutant mice

CCM2 was initially cloned via yeast-two-hybrid screens as an adaptor protein (termed OSM) for the 'Mitogen-Activated Protein Kinase Kinase Kinase 3' (MEKK3), a kinase capable of activating the transcription factor NF-κB (18–20) (unpublished data). Subsequently this gene was identified as one of the three genetic loci carrying inactivating mutations in one of its alleles in patients with the inherited form of the CCM disease (12,21). To study the function of CCM2 *in vivo*, we first generated conventional *Ccm2* knockout mice (Supplementary Material, Fig. S1A). To explore the role of CCM2 specifically in the vasculature during development, but also to explore CCM2's role in adults, we further generated conditional *Ccm2* knockout mice (Supplementary Material, Fig. S1B). On a C57BL/6J background, $Ccm2^{+/-}$ heterozygous mice, $Ccm2^{flox/+}$ heterozygous mice and $Ccm2^{flox/flox}$ homozygous mice are all viable and fertile.

$Ccm2^{-/-}$ homozygous mice were embryonic lethal and displayed cardiovascular defects, as previously reported (8–10). By E8.5–E9.5, homozygous embryos were clearly distinguishable from their wild-type or heterozygous littermates due to pericardial edema, a truncated forehead region, growth retardation and arrested heart development (Supplementary Material, Fig. S2). All mutant embryos observed were dead by E10.

Ccm2 is required for proper angiogenesis

The yolk sac vasculature is a prominent site of angiogenesis in the early embryo at E8.5–E9.5, where the primitive capillary vascular plexus rapidly remodels to form a well-defined, hierarchical branching network (Fig. 1A, arrowheads). E9.5 *Ccm2* homozygous mutant yolk sac displayed a complete lack of remodeled vessels, although the mutants appeared to retain the capillary plexus resulting from vasculogenesis (Fig. 1A). Further analysis of peripheral vasculature and heart development was carried out in the *Ccm2* mutants and control littermates (heterozygous embryos) by whole-mount staining for PECAM-1, a pan-endothelial cell marker. In the *Ccm2* mutant embryos, the head and intersomitic vasculature failed to assemble properly (Fig. 1B versus C and D versus E).

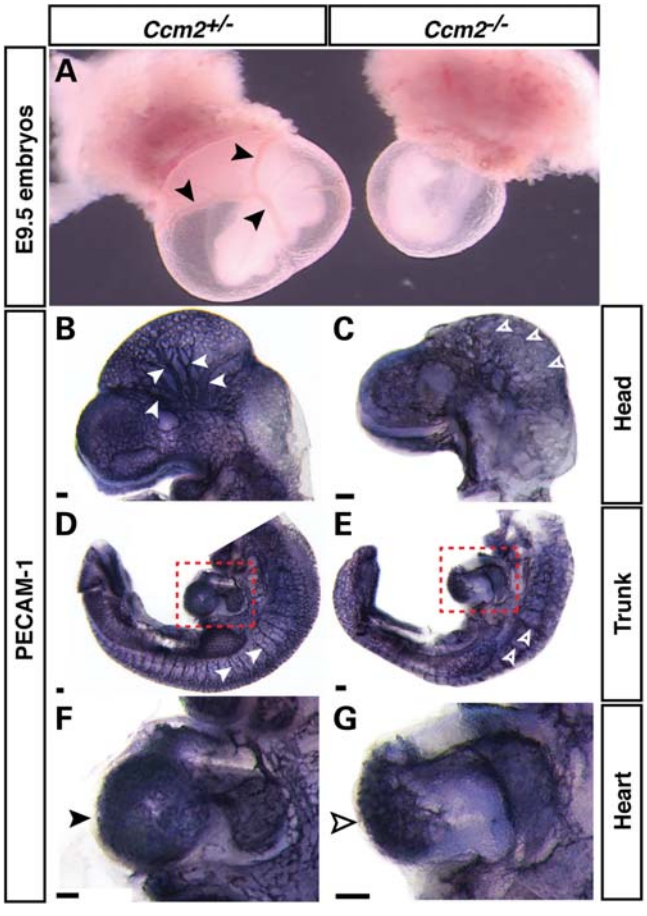

Figure 1. Cardiovascular defects in *Ccm2* mutant embryos. (**A**) Yolk sac angiogenesis is defective in *Ccm2* mutant embryos. Compared with the developing hierarchical vascular networks with remodeled vessels in the control $Ccm2^{+/-}$ yolk sac (arrowheads), the *Ccm2* mutant yolk sac reveals defective angiogenic remodeling. (**B** and **C**) Defective head angiogenesis in *Ccm2* mutant embryos. Whole-mount staining with a pan-endothelial cell marker, anti-PECAM-1 antibody shows arrested vascular remodeling in the head of *Ccm2* mutant embryos (open arrowheads) compared with littermate $Ccm2^{+/-}$ controls (arrowheads). (**D**–**G**) Defective trunk angiogenesis and heart morphogenesis in *Ccm2* mutant embryos. The remodeling of the intersomitic vessels seen in $Ccm2^{+/-}$ controls (D; arrowheads) is defective in *Ccm2* mutant embryos (F; open arrowheads). Growth of the ventricular endocardium appears arrested in *Ccm2* mutant embryos (G; open arrowhead) compared with controls (F; arrowhead) (red-dotted line enclosed boxes in D and E shown at higher magnification in F and G, respectively). Scale bars are 100 μm.

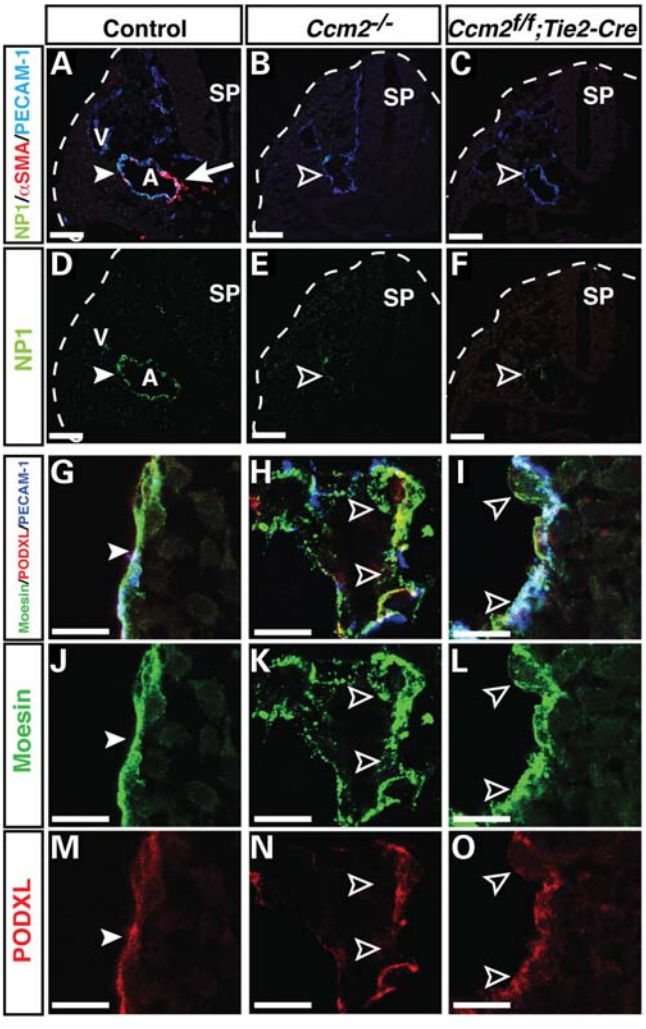

Figure 2. Defective arteriogenesis and vascular integrity in conventional and endothelial-specific *Ccm2* mutant embryos. (**A**–**F**) Triple immunofluorescence confocal microscopy using antibodies to the arterial markers NP1 (A–F, green), together with PECAM-1 (A–C, blue) and smooth muscle cell marker αSMA (A–C, red), as indicated. Both conventional mutant $Ccm2^{-/-}$ and endothelial-specific mutant $Ccm2^{flox/flox}$*; Tie2-Cre* embryos exhibit defective arterial differentiation when compared with controls ($Ccm2^{+/flox}$*; Tie2-Cre)* (A versus B and C, D versus E and F, arrowhead versus open arrowhead, respectively). In control littermates, αSMA^{+} SMCs are associated with the dorsal aorta (A) (red, arrow) but not with vein (V) at E9.5. In contrast, both $Ccm2^{-/-}$ and $Ccm2^{flox/flox}$*; Tie2-Cre* mutant embryos lack smooth muscle coverage in dorsal aorta (A versus B and C, red). Sp: spinal cord. Scale bars are 100 μm. (**G**–**O**) Triple immunofluorescence confocal microscopy of embryonic dorsal aorta was performed with antibodies to vascular luminal membrane proteins Podocarxyn (PODXL, red) and Moesin (green), together with PECAM-1. In control littermates, the apical surface marker Podocarxyn presents on the vascular lumen and ERM adaptor protein Moesin is localized at the luminal or apical membranes to help form a stable vascular lumen (G, J, M, arrowheads). In contrast, the *CCM2* mutant mice do not display a smooth and stable vascular lumen with proper enrichment of Podocarxyn and Moesin (H, I, K, L, N, O, open arrowheads). Between the two *CCM2* mutants, the conventional $Ccm2^{-/-}$ mutants display a greater disruption of the luminal surface than the $Ccm2^{flox/flox}$*; Tie2-Cre* mutants (H versus I, K versus L and N versus O). Scale bars are 100 μm.

By E9.5, control littermates had developed the fine branches of the head vasculature (Fig. 1B). In contrast, while the initial head capillary plexus had also formed in the homozygous mutants, it subsequently remained in a primitive state (Fig. 1C). The intersomitic vessels arise from branches of the dorsal aorta and posterior cardinal veins, and grow between adjacent somites to form an intricate network (Fig. 1D). In the homozygous mutants, the vessels appeared to fuse with little branching (Fig. 1E). These phenotypes indicate an angiogenic arrest during cardiovascular development, consistent with previous reports (8–10).

To explore whether endothelial CCM2 is required for the vascular development, we sought to conditionally knock out *Ccm2* in ECs. Deletion of *Ccm2* in ECs was accomplished with a *Tie2-Cre* driver, which is active in the endothelium (22). We observed growth arrest in $Ccm2^{flox/flox}$*;Tie2-Cre* embryos compared with control littermates, although the arrest was less severe than that of conventional *CCM2*

knockouts (data not shown). The head and trunk of such embryos were subjected to whole-mount analysis with anti-PECAM-1 antibody. *Ccm2$^{flox/flox}$;Tie2-Cre* embryos failed to properly remodel the vasculature to form a hierarchical branching network in yolk sacs, and head and intersomitic regions (Supplementary Material, Fig. S3A and C versus B and D), identical to what had been observed in conventional *Ccm2* homozygous embryos. Taken together, these data suggest that endothelial *Ccm2* is essential for embryonic angiogenesis, in agreement with prior reports (8,9).

We further examined the development of the dorsal aorta in the conventional and conditional *Ccm2* mutant embryos. By E9.5, dorsal aorta formed with the expression of arterial markers (Fig. 2A and D). The expression of the arterial EC marker NP1 was greatly reduced in the dorsal aorta of both *Ccm2* homozygous and *Ccm2$^{flox/flox}$;Tie2-Cre* embryos (Fig. 2B, C, E, F). These data suggest that arteriogenesis is deficient in the *Ccm2* mutant embryos.

Defective vascular integrity in *Ccm2* mutant embryos

The fact that human CCM lesions displayed a disrupted endothelial lumen devoid of smooth muscle coverage that resulted in intracranial hemorrhage prompted us to examine whether the *Ccm2* mutant vessels recruit vascular SMCs and form proper endothelial junctions and lumen. By E9.5, dorsal aortae were associated with αSMA$^+$ vascular SMCs in the littermate control embryos (Fig. 2A). In contrast, αSMA$^+$ vascular SMCs were not detectable in the aortae of either *Ccm2* homozygous or *Ccm2$^{flox/flox}$;Tie2-Cre* embryos (Fig. 2B and C). Because endothelial cell-specific deletion of *Ccm2* resulted in defective smooth muscle coverage, this suggests that CCM2-deficient ECs were defective in the recruitment of these cells. We next examined the distribution of the luminal surface marker Podocarxyn (PODXL) and the Ezrin–Radixin–Moesin adaptor protein, both of which localize to endothelial cell–cell contacts and are enriched at the plasma membrane facing the developing vascular lumen (23). We found that the conventional and EC conditional *Ccm2* mutant embryos failed to form a proper aortic lumen; deletion of *Ccm2* resulted in a disrupted lumen compared with what was observed in control littermates (Fig. 2G versus H; I and J versus K; L and M versus N and O). These results indicate that Ccm2 function is required for proper endothelial lumen formation.

Ccm2 function is required for heart development

We first carefully assessed the cardiac phenotype of *Ccm2* mutants by using whole-mount staining with anti-PECAM-1 antibody. Obvious defects in cardiac morphogenesis were seen in both *Ccm2* homozygous and *Ccm2$^{flox/flox}$;Tie2-Cre* embryos (Fig. 1F versus G and Supplementary Material, Fig. S3E versus F). The cardiac looping was incomplete and the PECAM-1$^+$ endocardium failed to expand. These findings were confirmed by analysis of the endocardium in stained sections which revealed that the *Ccm2* mutant hearts had no or significantly deficient ventricular trabeculation (Supplementary Material, Fig. S4A versus B and C; D versus E and F).

Conditional deletion of *Ccm2* leads to hemorrhage in the adult brain

Since conventional or endothelial-specific deletion of *Ccm2* resulted in embryonic lethality, these mice do not represent models for the human disease, which occurs in mid-life and which is characterized by lesions largely confined to capillaries in brains. However, the cardiovascular defects detected in early embryos did prompt us to generate *Ccm2$^{flox/flox}$;MX1-Cre* mice, because such mice afforded us the opportunity to conditionally delete the *Ccm2* gene in adult tissues, and thus test whether deletions in adults might cause brain hemorrhages as seen in the human CCM disease. Previous studies indicated that brain ECs are an efficient target for the *MX1-Cre*-mediated inducible knockout system (24,25). In agreement with this, we found that the Cre expression is mainly detected in PECAM-1$^+$ ECs but not GFAP$^+$ glial cells in the brain of polyinosinic–polycytidylic acid (pIpC)-treatment of *Ccm2$^{flox/flox}$;MX1-Cre* mice (Supplementary Material, Fig. S5, arrowheads). We treated *Ccm2$^{flox/flox}$;MX1-Cre* mice and *Ccm2$^{flox/+}$;MX1-Cre* control littermates with three injections of pIpC at 2-day intervals to induce *Cre* expression in 6–8-week-old mice. We did not observe any apparent neurologic or other defects during the first couple of months, during which we inspected mice regularly. However, between 7 and 8 months of age, three out of six *Ccm2$^{flox/flox}$;MX1-Cre* mice suddenly and unexpectedly died, while none of the littermate controls suffered this fate; these events prompted us to again more closely observe the remaining pIpC-treated *Ccm2$^{flox/flox}$;MX1-Cre* mice. Within a week, we noted that one of these mice had developed a pronounced ataxia with seizure-like behavior. At this juncture, we euthanized all remaining *Ccm2$^{flox/flox}$;MX1-Cre* pIpC-treated mice as well as their littermate controls and performed histological analyses of their brains. Gross inspection of whole brains demonstrated that all *flox/flox* mutant, pIpC-treated mice exhibited prominent hemorrhages, while none of the littermate controls (*flox/+*; pIpC-treated) exhibited such lesions (Fig. 3A versus B, dorsal view; C versus D, ventral view). It is thus likely that the sudden deaths of the first three pIpC-treated *Ccm2$^{flox/flox}$;MX1-Cre* were due also to hemorrhages and associated neurologic defects.

Further analyses of sections revealed that hemorrhages appeared widespread throughout the brain, with larger hemorrhages visible most often in the cerebrum and cerebellum (Fig. 3F and H, respectively; littermate controls Fig. 3E and G). This mosaic phenotype might reflect either the efficiency of *Cre*-mediated deletion of *Ccm2* or the contribution of *Ccm2*-deficient circulating endothelial progenitors to the brain microvasculature (see Discussion). H&E and Nissl stainings confirmed hemorrhages and also showed damaged neuronal architecture in the cerebrum (H&E, Fig. 4A and C versus B and D; Nissl, Fig. 4E and G versus F and H) and cerebellum (H&E, Supplementary Material, Fig. S6A and C versus B and D; Nissl, Fig. S6E and G versus F and H) of pIpC-treated *Ccm2$^{flox/flox}$;MX1-Cre* mouse brains. Consistent with the fact that magnetic resonance imaging detects iron deposits in CCM lesions in patients, we also observed the accumulation of hemosiderin, a breakdown product of erythrocytes, as evidenced by brown granules in the affected mice (Fig. 4D,

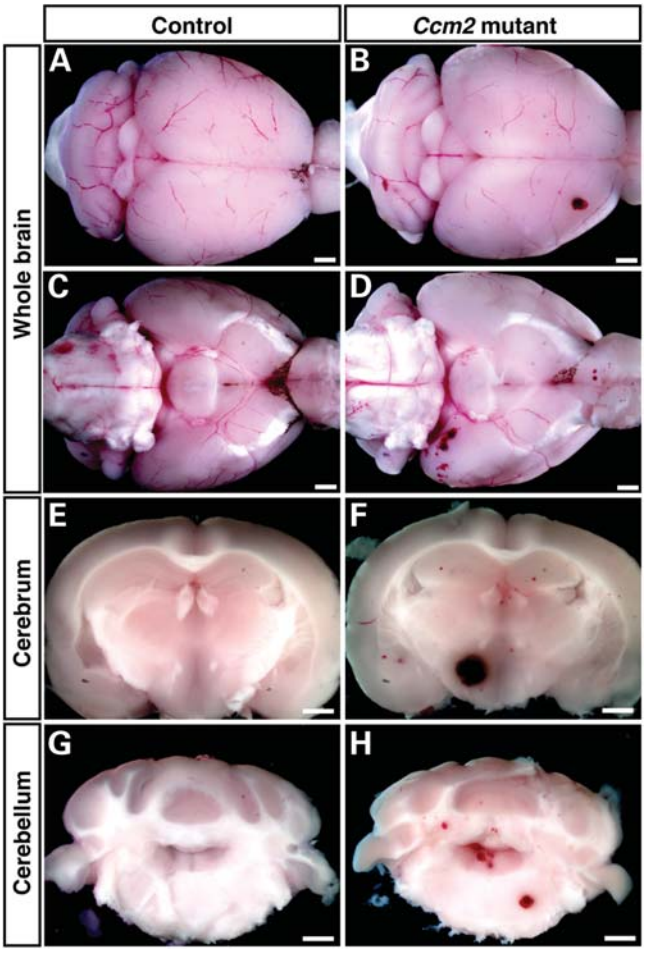

Figure 3. Brain hemorrhage in inducibly deleted, adult *Ccm2* mutant mice. Gross view and coronal sections are shown. Brain lesions are detected in the cerebrum and cerebellum of 7–8 months-old, polyinosinic–polycytidylic acid (pIpC)-treated $Ccm2^{flox/flox}$;*MX1-Cre* mice (**B**, **D**, **F**, **H**), but not in similarly treated $Ccm2^{flox/+}$;*MX1-Cre* control littermates (**A**, **C**, **E**, **G**). Scale bars are 1 mm.

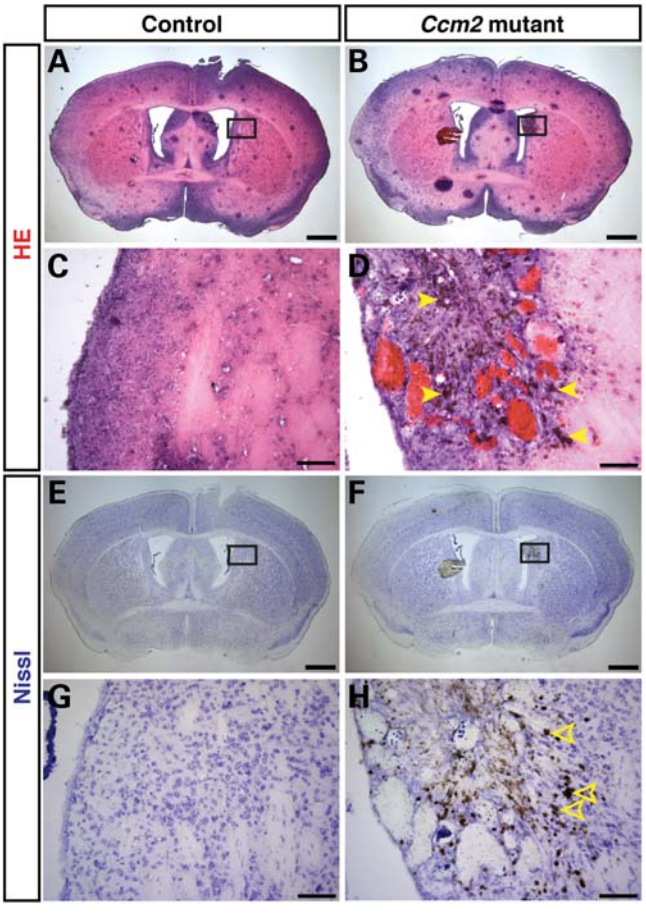

Figure 4. Widespread hemorrhage in the cerebrum of inducibly deleted, adult *Ccm2* mutant mice. (**A**–**D**) H&E stainings of coronal sections reveal that pIpC-treated $Ccm2^{flox/flox}$;*MX1-Cre* mice have dilated vessels and hemorrhage with accumulation of hemosiderin, a breakdown product of erythrocytes, as evidenced by brown granules (arrowheads; representative stained deposits). (**E**–**H**) Nissl stainings of coronal sections reveal that pIpC-treated $Ccm2^{flox/flox}$;*MX1-Cre* mice have damaged neuronal architecture in the lesion (open arrowheads; representative damaged neurons) when compared with the pIpC-treated control littermates. The boxed areas in (E) and (F) are shown at higher magnification in (G) and (H). Scale bars: A, B, E, F are 1 mm; C, D, G, H are 100 μm.

arrowheads). Damaged neurons were only seen in the CCM lesion (Fig. 4H, open arrowheads). In contrast, we did not find any neurological defects or hemorrhages in the control littermates of the same age. These findings demonstrate that conditional deletion of *Ccm2* in adult mice results in hemorrhages in the adult brain, which likely cause neuronal damage and, in consequence, visible neurologic defects, such as ataxia, and ultimately death.

We further addressed whether the brain lesions underlying hemorrhage have defective vascular integrity; specifically, we investigated lumen formation. We found that normal capillaries present in both pIpC-treated $Ccm2^{flox/flox}$;*MX1-Cre* mice and their control littermates had a grossly normal Podocarxyn $(PODXL)^+$ lumen structure (Fig. 5D and E). In contrast, the lesional, CCM-like vessels showed massive accumulation of $Ter119^+$ erythrocytes, were grossly dilated and exhibited an impaired and disrupted endothelial lumen structure (Fig. 5B, C, F and G; littermate control 5A); the lesional vessels were apparently prone to rupture, resulting in hemorrhage, as evidenced by erythrocytes outside the vessels (Fig. 5B and G). In addition, $CD11b^+$ microglia were recruited to CCM lesions (Fig. 6C versus D), where dilated vessels and damaged vessels without extracellular matrix were present (Fig. 6B; littermate control 6A). This suggests an immune response to the CCM pathology (Fig. 6D). Furthermore, $GFAP^+$ astrocytes failed to extend their projections to surround capillaries (Fig. 6E versus F). In addition, only very few or no $Aquaporin4^+$ astrocyte end-feet could be detected in CCM lesions (Supplementary Material, Fig. S7). Instead, $GFAP^+$ astrocytes formed abnormal cell clusters in the vicinity of the lesional vessels (Fig. 6F, arrowheads). Such findings indicate an impaired blood–brain barrier in the CCM lesions. The observed pathological features of the brain lesions in the pIpC-treated $Ccm2^{flox/flox}$;*MX1-Cre* mice appear to be highly similar to those described for lesions in human CCM patients (reviewed in 2,26). We also investigated $Ccm2^{flox/flox}$;*MX1-Cre* just 3 weeks after pIpC-treatment and were able to detect lesions already at this early time point, although these

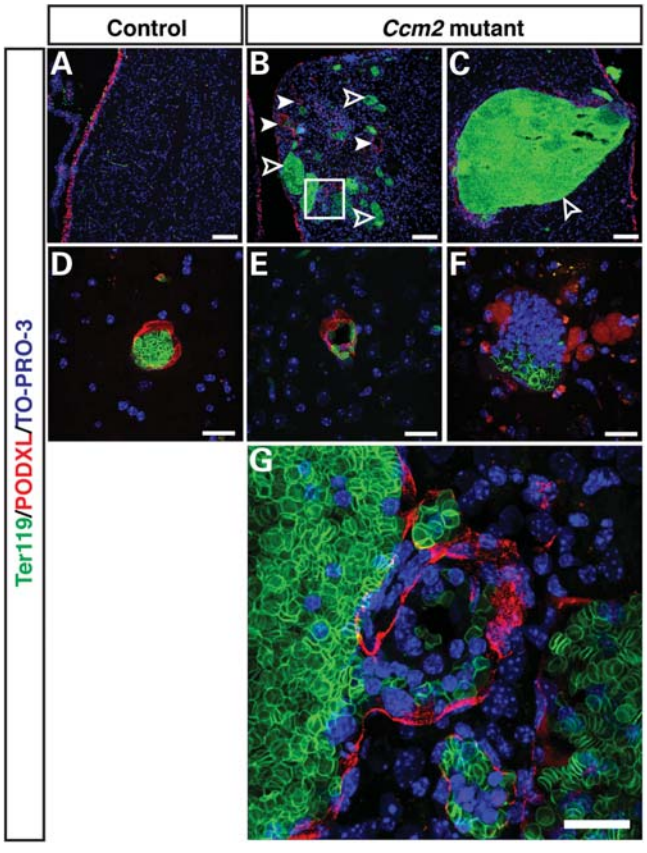

Figure 5. Vessel dilation and lumen breakdown in the cerebrum of the inducibly deleted, adult *Ccm2* mutant mice. Triple immunofluorescence confocal microscopy of coronal sections was performed with antibodies to a vascular lumen marker Podocarxyn (PODXL) (red), together with the erythrocyte marker Ter119 (green) and the pan-nuclear marker TO-PRO-3 (blue). The pIpC-treated $Ccm2^{flox/flox}$;*MX1-Cre* mice have dilated vessels (**B**, arrowheads), and damaged vessels which failed to form a proper vascular lumen (B, open arrowhead; **C** and **F**) in hemorrhaged areas (CCM-like lesions),while the pIpC-treated control littermates have only normal-sized vessels with well-demarcated lumen (**A** and **D**). Normal capillaries are also present in $Ccm2^{flox/flox}$;*MX1-Cre* mice in areas that do not show any hemorrhage (**E**). The boxed region in (B) is shown at higher magnification in (**G**). The vascular lumen appears to have ruptured resulting in hemorrhage, as evidenced by erythrocytes outside the vessel enclosure. Scale bars: A, B, C are 100 μm; D, E, F, G are 20 μm.

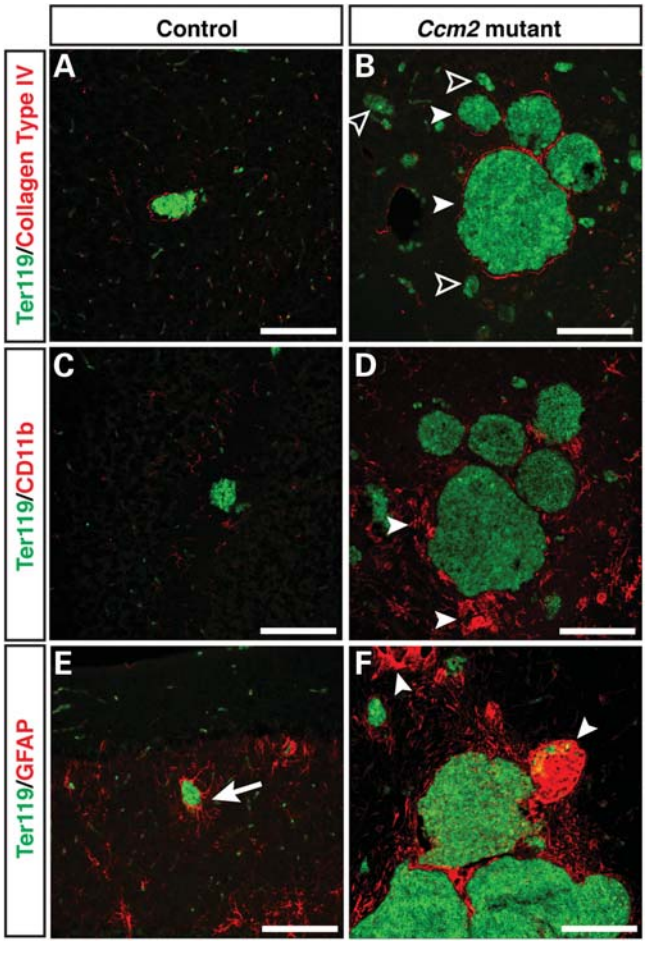

Figure 6. CCM-like lesions are associated with an immune response and exhibit damaged neuro-vascular units. Double immunofluorescence confocal microscopy of coronal sections was performed using antibodies to either collagen type IV (**A** and **B**, red), microglia and macrophage marker CD11b (C and D, red) or astrocyte marker GFAP (E and F, red) together with Ter119 (green). (A and B) The pIpC-treated $Ccm2^{flox/flox}$;*MX1-Cre* mice have collagen type IV^+ dilated vessels (B, arrowheads) and collagen type4$^-$ damaged vessels (B, open arrowheads). Control littermates only have normal-sized collagen type IV^+ vessels (A). (**C** and **D**) Increased numbers of $CD11b^+$ microglia or macrophages are seen in the CCM-like lesions (D, arrowheads). (**E** and **F**) $GFAP^+$ astrocytes interact with capillaries in littermate controls to help form the neurovascular unit that establishes the blood brain barrier (E, arrow). In areas containing CCM-like lesions in mutant mice, the neurovascular unit appears to be disrupted and abnormal aggregations of $GFAP^+$ cells are evident (F, arrowheads). Scale bars are 20 μm.

lesions appeared to be mostly smaller (Supplementary Material, Fig. S8). Taken together, our results demonstrate that conditional deletion of *Ccm2* in adult mice causes CCM-like lesions with hemorrhage in the brain, which can result in significant neurologic defects and ultimately death with advancing age.

DISCUSSION

Loss-of-function mutations of *Ccm* genes in humans can lead to lesions in brain capillaries that result in hemorrhages that in turn cause apparent neurologic defects and even death in patients. However, the roles of CCM proteins in brain vasculature and their significance in the disease context have remained poorly understood. In the present study, we first provide genetic evidence that endothelial and/or endocardial *Ccm2* expression in mice is required for proper angiogenesis and heart development during embryogenesis, in agreement with previous studies (8–10). We have extended these observations to show that expression of *Ccm2* in ECs is required for formation of smooth and stable vessel lumens, implying a role for CCM2 in endothelial cell–cell interactions. Importantly, we now demonstrate that conditional *Ccm2* gene inactivation in adult mice induces brain hemorrhages highly reminiscent of those observed in human CCM patients. This provides the first CCM2 mouse model for CCMs. The CCM-like brain lesions induced in mice display disrupted vascular lumens and enlarged capillary cavities, lacking neuro-vascular associations; in addition, these lesions are surrounded by accumulations of activated microglia. This CCM animal model should prove to be very valuable to explore the signaling pathways and functions

of CCM2 and to understand how the absence of CCM2 can lead to severe CCMs in brain capillaries. Furthermore, this animal model may prove useful in testing therapeutic intervention strategies for the human disease.

Our data demonstrate that CCM2 is required in endothelium for the angiogenic remodeling of the vasculature in the yolk sac, the head and intersomitic vessels, but is not required for the initial primary capillary formation. We also find that expression of arterial markers and recruitment of vascular SMCs are severely impaired in *Ccm2* mutants. Previous studies by others and us have indicated that VEGF-A induces arterial differentiation by acting through the Notch pathway (27–29). Furthermore, VEGF-A has also recently been shown to stabilize VEGR2 via CCM3, thereby facilitating signaling by this receptor (11). Given the ability of CCM2 to associate with both CCM1 and CCM3, CCM2 could conceivably have a role in VEGFR2 signaling as well.

Complete lumen formation in the dorsal aorta is essential for a proper circulatory system. Our extensive confocal imaging analyses, which have made use of several markers for luminal membranes, have revealed that deletion of endothelial *Ccm2* resulted in a disrupted lumen in dorsal aorta. This observation suggests that CCM2 may regulate cytoskeletal architecture in ECs. Recent biochemical studies using human microvascular endothelial cells indicate that CCM2 can directly associate with and inhibit RhoA activity, decreasing stress fiber formation; therefore, loss of *Ccm2* could lead to disruption of cell–cell junctions and thus lumen formation as a consequence of cytoskeletal changes (9).

During heart development, essential and reciprocal interactions occur between endocardial cells and between endocardial and myocardial cells. Notch has been shown to mediate the endocardium–myocardium interaction that is critical for trabeculation and ventricular chamber morphogenesis (30). Interestingly, endothelial/endocardial deletion of *Notch1* or *RBPJk* results in defective ventricular patterning and trabeculation that is almost identical to the cardiac phenotype seen in the *Ccm2* mutants. A recent report also demonstrates that CCM1 may activate Delta–Notch signaling, which leads to AKT phosphorylation in ECs *in vitro* (31).

The induced loss of *Ccm2* in a limited number of blood-accessible cells and ECs in adult mice generated specific, localized lesions in brain capillaries, resulting over time in neurologic defects, hemorrhages and ultimately the death of animals. The lesions observed in the *Ccm2* mutants appear to be very similar to those seen in human CCM patients. Mouse brain lesions were characterized by grossly dilated malformed vessels that were prone to rupture, releasing erythrocytes. Furthermore, the normal EC–astrocyte interaction was severely disrupted. These findings indicate defects in EC association of the lesional vessels that are somewhat reminiscent of those seen during angiogenesis in mice lacking CCM2 in ECs during embryonic development. Similar to human lesions, those in brains of adult mice were associated with an immune response as well, as documented by the recruitment of microglia.

How might loss of CCM2 cause lesions in adult brain? Since only a small subset of brain capillaries develops malformations and hemorrhages, we hypothesize that such lesions may develop in newly forming vessels, a process that may be initiated in response to local inflammation or some other event (32,33). If so, one may imagine a scenario, wherein resident *Ccm2*-deleted ECs and/or EC precursors are recruited into newly sprouting vessels, resulting in a partially defective/disrupted lumen on account of the impaired functions of the *Ccm2*-deficient ECs. In an alternative and possibly additional scenario, one may imagine that mutant resident ECs and/or their precursors may be prone to initiate new vessel formation and/or preferentially contribute after the process has been initiated, thus increasing the representation of mutant cells in the new vessel wall. In support of this hypothesis, recent reports have suggested that loss of CCM proteins might in fact promote angiogenic sprouting, migration and proliferation of ECs in culture (31,34–36). Conceivably, CCM proteins could have a positive role in transmitting angiogenic signals, while at the same time, setting thresholds to limit spontaneous growth and sprouting.

The brain lesions induced by pIpC-treatment of $Ccm2^{flox/flox}$;*MX1-Cre* mice over time appear to faithfully recapitulate the pathogenesis of the lesions in human CCM patients. Therefore, this represents the first CCM2 mouse model for the CCM disease. After completion of our work, another mouse model for CCM was recently reported (37). In this model, heterozygous $Ccm1^{+/-}$ mice were crossed onto a background of *Msh2* deficiency, a gene critical for mismatch repair. In this model, complete loss of *Ccm1* was suggested to occur in some cells as a result of the increased somatic mutational load, resulting in brain lesions resembling those seen in human patients. In contrast, backcrossing of $Ccm2^{+/-}$ mice onto an *Msh2* deficient background failed to generate lesions; the reasons for this are unknown. Unlike our model, wherein we induce the loss of *Ccm2* in adult mice, the timing of the deletion of *Ccm1* in the *Msh2*-deficient model cannot be controlled and loss of *Ccm1* and the generation of lesions could occur at any time starting during embryonic development; furthermore, penetrance in this model was reported at 50% only. Finally, and importantly, *Msh2* deficiency likely predisposes towards mutations in other genes, which potentially compromises the usefulness of the model. Nevertheless, the two models are also complementary as they provide a means to compare and contrast the pathogenesis of lesions induced by loss of two different CCM proteins; CCM proteins may have distinct activities in the context of CCMs (36).

The pIpC-induced, *MX1-Cre*-mediated deletion of *Ccm2* in adult mice described here represents a temporally controllable and fully penetrant model for generating brain vascular lesions that resemble those observed in human CCM patients. This mouse disease model should greatly facilitate further investigations into the cellular and molecular mechanisms underlying CCM vascular disease and may ultimately allow for testing of possible therapeutic interventions to slow or stop the progression of this disease.

MATERIALS AND METHODS

Mice

Conventional and conditional *Ccm2* knockout mice on the C57BL/6 (B6) background were generated by homologous

recombination in ES cells according to standard procedures (see Supplementary Material, Fig. S1A and B). Knockout founder mice were generated at Ozgene (Ozgene Pty Ltd, Bentley, Western Australia, Australia). *Tie2-Cre* (22) and *MX1-Cre* (38) mice have been described elsewhere and were crossed with the conditional *CCM2* knockout mice. Mice were bred and housed in National Institute of Allergy and Infectious Diseases (NIAID) facilities, and all experiments were done with approval of the NIAID Animal Care and Use Committee and in accordance with all relevant institutional guidelines.

Whole-mount and section immunohistochemistry of mouse embryo

Mouse embryos were dissected between E8.5 and E9.5, fixed in 4% paraformaldehyde/PBS at 4°C for 1–2 h. Staining was performed using anti-PECAM-1 antibody (rat monoclonal antibody, clone MEC 13.3, BD pharmingen, 1:300, overnight at 4°C) to detect endothelial/endocardial cells. HRP-conjugated secondary antibody (Jackson, 1:300, overnight at 4°C) was then used. All brightfield images were captured using QImaging RETIGA 2000R camera (QImaging). For section staining, fixed embryos were sunk in 15% sucrose and 7.5% gelatin in PBS, and then 10 μm sections were collected on a cryostat (Leica). Staining was performed using anti-PECAM-1 antibody (rat monoclonal antibody, clone MEC 13.3, BD pharmingen, 1:300, overnight at 4°C or hamster monoclonal antibody, Chemicon, 1:200, overnight at 4°C) to detect endothelial/endocardial cells, and an anti-NP1 antibody (rabbit polyclonal antibody, A.L. Kolodkin, 1:3000, 3 h at room temperature) as an arterial marker; Cy3-conjugated anti-αSMA antibody to detect SMCs; anti-Moesin antibody (rabbit polyclonal antibody, Abcam, 1:200, overnight at 4°C) and anti-Podocarxyn antibody (rat monoclonal antibody, R&D, 1:200, overnight at 4°C) as vascular lumen markers. TO-PRO-3 (Invitrogen, 1:1000, 10 min at room temperature) was used as a pan-nuclear marker. For immunofluorescent detection, Alexa-488-, Alexa-568-, Alexa-633 or Cy5-conjugated secondary antibodies (Invitrogen, 1:250, and Jackson, 1:300, 1 h at room temperature) were used. All confocal microscopy was carried out on a Leica SP5 confocal (Leica).

Histology of adult brain

All brightfield images of whole and sectioned brains were captured using QImaging RETIGA 2000R camera (QImaging). For brain-section staining, brains were fixed in 4% paraformaldehyde/PBS at 4°C for overnight, sunk in 15% sucrose in PBS and then 20 μm sections were collected on a cryostat (Leica). Staining was performed using anti-Ter119 antibody (rat monoclonal antibody, BD pharmingen, 1:300, overnight at 4°C) to detect erythrocytes, anti-Podocarxyn antibody to detect vascular lumen, anti-collagen type IV antibody (rabbit polyclonal antibody, AbD Serotec, 1:300, overnight at 4°C) to detect ECs, anti-CD11b antibody (rat monoclonal antibody, clone M1/70.15, AbD Serotec, 1:200, overnight at 4°C) to detect microglia, anti-GFAP antibody (rabbit polyclonal antibody, DAKO, 1:200, overnight at 4°C) and anti-Aquaporin4 antibody (rabbit polyclonal antibody, Millipore, 1:500, overnight at 4°C) to detect astrocytes and anti-Cre antibody (mouse IgG1 monoclonal antibody, D.J. Anderson, 1:100, overnight at 4°C). TO-PRO-3 was used as a pan-nuclear marker. For immunofluorescent detection, Alexa-488-, Alexa-568-, Alexa-633 (Invitrogen, 1:250, 1 h at room temperature) were used. All confocal microscopy was carried out on a Leica SP5 confocal (Leica). H&E and Nissl stainings of coronal sections were performed and images were captured using QImaging RETIGA 2000R camera (QImaging).

pIpC administration

$Ccm2^{flox/flox}$and $Ccm2f^{lox/+}$ mice carrying the *MX1-Cre* transgene were injected with 250 μg pIpC (Sigma-Aldrich, St Louis, MO) three times at 2-day intervals.

SUPPLEMENTARY MATERIAL

Supplementary Material is available at *HMG* online.

ACKNOWLEDGEMENTS

We thank K. Gill for laboratory management, Y. Carter for administrative assistance and C. Li for technical help. We are grateful to Dr A.S. Fauci for continued support. We also thank Mukouyama and Siebenlist lab members for technical help and discussion.

Conflict of Interest statement. None declared.

FUNDING

This work was supported by funding from the Intramural Research Programs of the National Institute of Allergy and Infectious Diseases and the National Heart, Lung, and Blood Institute, National Institutes of Health, Bethesda, MD, USA.

REFERENCES

1. Riant, F., Bergametti, F., Ayrignac, X., Boulday, G. and Tournier-Lasserve, E. (2010) Recent insights into cerebral cavernous malformations: the molecular genetics of CCM. *FEBS. J.*, **277**, 1070–1075.
2. Chan, A.C., Li, D.Y., Berg, M.J. and Whitehead, K.J. (2010) Recent insights into cerebral cavernous malformations: animal models of CCM and the human phenotype. *FEBS. J.*, **277**, 1076–1083.
3. Gault, J., Shenkar, R., Recksiek, P. and Awad, I.A. (2005) Biallelic somatic and germ line CCM1 truncating mutations in a cerebral cavernous malformation lesion. *Stroke*, **36**, 872–874.
4. Gault, J., Awad, I.A., Recksiek, P., Shenkar, R., Breeze, R., Handler, M. and Kleinschmidt-DeMasters, B.K. (2009) Cerebral cavernous malformations: somatic mutations in vascular endothelial cells. *Neurosurgery*, **65**, 138–144.
5. Akers, A.L., Johnson, E., Steinberg, G.K., Zabramski, J.M. and Marchuk, D.A. (2009) Biallelic somatic and germline mutations in cerebral cavernous malformations (CCMs): evidence for a two-hit mechanism of CCM pathogenesis. *Hum. Mol. Genet.*, **18**, 919–930.
6. Pagenstecher, A., Stahl, S., Sure, U. and Felbor, U. (2009) A two-hit mechanism causes cerebral cavernous malformations: complete inactivation of CCM1, CCM2 or CCM3 in affected endothelial cells. *Hum. Mol. Genet.*, **18**, 911–918.
7. Whitehead, K.J., Plummer, N.W., Adams, J.A., Marchuk, D.A. and Li, D.Y. (2004) Ccm1 is required for arterial morphogenesis: implications for

the etiology of human cavernous malformations. *Development*, **131**, 1437–1448.
8. Boulday, G., Blécon, A., Petit, N., Chareyre, F., Garcia, L.A., Niwa-Kawakita, M., Giovannini, M. and Tournier-Lasserve, E. (2009) Tissue-specific conditional CCM2 knockout mice establish the essential role of endothelial CCM2 in angiogenesis: implications for human cerebral cavernous malformations. *Dis. Model. Mech.*, **2**, 168–177.
9. Whitehead, K.J., Chan, A.C., Navankasattusas, S., Koh, W., London, N.R., Ling, J., Mayo, A.H., Drakos, S.G., Jones, C.A., Zhu, W. *et al.* (2009) The cerebral cavernous malformation signaling pathway promotes vascular integrity via Rho GTPases. *Nat. Med.*, **15**, 177–184.
10. Kleaveland, B., Zheng, X., Liu, J.J., Blum, Y., Tung, J.J., Zou, Z., Sweeney, S.M., Chen, M., Guo, L., Lu, M.M. *et al.* (2009) Regulation of cardiovascular development and integrity by the heart of glass-cerebral cavernous malformation protein pathway. *Nat. Med.*, **15**, 169–176.
11. He, Y., Zhang, H., Yu, L., Gunel, M., Boggon, T.J., Chen, H. and Min, W. (2010) Stabilization of VEGFR2 signaling by cerebral cavernous malformation 3 is critical for vascular development. *Sci. Signal.*, **3**, ra26.
12. Denier, C., Goutagny, S., Labauge, P., Krivosic, V., Arnoult, M., Cousin, A., Benabid, A.L., Comoy, J., Frerebeau, P., Gilbert, B. *et al.* (2004) Mutations within the MGC4607 gene cause cerebral cavernous malformations. *Am. J. Hum. Genet.*, **74**, 326–337.
13. Plummer, N.W., Squire, T.L., Srinivasan, S., Huang, E., Zawistowski, J.S., Matsunami, H., Hale, L.P. and Marchuk, D.A. (2006) Neuronal expression of the Ccm2 gene in a new mouse model of cerebral cavernous malformations. *Mamm. Genome.*, **17**, 119–128.
14. Louvi, A., Chen, L., Two, A.M., Zhang, H., Min, W. and Gunel, M. (2011) Loss of cerebral cavernous malformation 3 (Ccm3) in neuroglia leads to CCM and vascular pathology. *Proc. Natl Acad. Sci. USA.*, **108**, 3737–3742.
15. Clatterbuck, R.E., Eberhart, C.G., Crain, B.J. and Rigamonti, D. (2001) Ultrastructural and immunocytochemical evidence that an incompetent blood-brain barrier is related to the pathophysiology of cavernous malformations. *J. Neurol. Neurosurg. Psychiatry*, **71**, 188–192.
16. Faurobert, E. and Albiges-Rizo, C. (2010) Recent insights into cerebral cavernous malformations: a complex jigsaw puzzle under construction. *FEBS. J.*, **277**, 1084–1096.
17. Plummer, N.W., Gallione, C.J., Srinivasan, S., Zawistowski, J.S., Louis, D.N. and Marchuk, D.A. (2004) Loss of p53 sensitizes mice with a mutation in Ccm1 (KRIT1) to development of cerebral vascular malformations. *Am. J. Pathol.*, **165**, 1509–1518.
18. Uhlik, M.T., Abell, A.N., Johnson, N.L., Sun, W., Cuevas, B.D., Lobel-Rice, K.E., Horne, E.A., Dell'Acqua, M.L. and Johnson, G.L. (2003) Rac-MEKK3-MKK3 scaffolding for p38 MAPK activation during hyperosmotic shock. *Nat. Cell. Biol.*, **5**, 1104–1110.
19. Ellinger-Ziegelbauer, H., Brown, K., Kelly, K. and Siebenlist, U. (1997) Direct activation of the stress-activated protein kinase (SAPK) and extracellular signal-regulated protein kinase (ERK) pathways by an inducible mitogen-activated protein Kinase/ERK kinase kinase 3 (MEKK) derivative. *J. Biol. Chem.*, **272**, 2668–2674.
20. Ellinger-Ziegelbauer, H., Kelly, K. and Siebenlist, U. (1999) Cell cycle arrest and reversion of Ras-induced transformation by a conditionally activated form of mitogen-activated protein kinase kinase kinase 3. *Mol. Cell. Biol.*, **19**, 3857–3868.
21. Liquori, C.L., Berg, M.J., Siegel, A.M., Huang, E., Zawistowski, J.S., Stoffer, T., Verlaan, D., Balogun, F., Hughes, L., Leedom, T.P. *et al.* (2003) Mutations in a gene encoding a novel protein containing a phosphotyrosine-binding domain cause type 2 cerebral cavernous malformations. *Am. J. Hum. Genet.*, **73**, 1459–1464.
22. Kisanuki, Y.Y., Hammer, R.E., Miyazaki, J., Williams, S.C., Richardson, J.A. and Yanagisawa, M. (2001) Tie2-Cre transgenic mice: a new model for endothelial cell-lineage analysis *in vivo*. *Dev. Biol.*, **230**, 230–242.
23. Strilić, B., Kucera, T., Eglinger, J., Hughes, M.R., McNagny, K.M., Tsukita, S., Dejana, E., Ferrara, N. and Lammert, E. (2009) The molecular basis of vascular lumen formation in the developing mouse aorta. *Dev. Cell.*, **17**, 505–515.
24. Schneider, A., Zhang, Y., Guan, Y., Davis, L.S. and Breyer, M.D. (2003) Differential, inducible gene targeting in renal epithelia, vascular endothelium, and viscera of Mx1Cre mice. *Am. J. Physiol. Renal. Physiol.*, **284**, F411–F417.
25. Hayashi, M., Kim, S.W., Imanaka-Yoshida, K., Yoshida, T., Abel, E.D., Eliceiri, B., Yang, Y., Ulevitch, R.J. and Lee, J.D. (2004) Targeted deletion of BMK1/ERK5 in adult mice perturbs vascular integrity and leads to endothelial failure. *J. Clin. Invest.*, **113**, 1138–1148.
26. Labauge, P., Denier, C., Bergametti, F. and Tournier-Lasserve, E. (2007) Genetics of cavernous angiomas. *Lancet. Neurol.*, **6**, 237–244.
27. Lawson, N.D., Scheer, N., Pham, V.N., Kim, C.H., Chitnis, A.B., Campos-Ortega, J.A. and Weinstein, B.M. (2001) Notch signaling is required for arterial-venous differentiation during embryonic vascular development. *Development*, **128**, 3675–3683.
28. Lawson, N.D., Vogel, A.M. and Weinstein, B.M. (2002) Sonic hedgehog and vascular endothelial growth factor act upstream of the Notch pathway during arterial endothelial differentiation. *Dev. Cell.*, **3**, 127–136.
29. Mukouyama, Y.S., Gerber, H.P., Ferrara, N., Gu, C. and Anderson, D.J. (2005) Peripheral nerve-derived VEGF promotes arterial differentiation via neuropilin 1-mediated positive feedback. *Development*, **132**, 941–952.
30. Grego-Bessa, J., Luna-Zurita, L., del Monte, G., Bolós, V., Melgar, P., Arandilla, A., Garratt, A.N., Zang, H., Mukouyama, Y.S., Chen, H. *et al.* (2007) Notch signaling is essential for ventricular chamber development. *Dev. Cell.*, **12**, 415–429.
31. Wüstehube, J., Bartol, A., Liebler, S.S., Brütsch, R., Zhu, Y., Felbor U., Sure, U., Augustin, H.G. and Fischer, A. (2010) Cerebral cavernous malformation protein CCM1 inhibits sprouting angiogenesis by activating DELTA-NOTCH signaling. *Proc. Natl Acad. Sci. USA.*, **107**, 12640–12645.
32. Lim, M., Cheshier, S. and Steinberg, G.K. (2006) New vessel formation in the central nervous system during tumor growth, vascular malformations, and Moyamoya. *Curr. Neurovasc. Res.*, **3**, 237–245.
33. Beck, H. and Plate, K.H. (2009) Angiogenesis after cerebral ischemia. *Acta. Neuropathol.*, **117**, 481–496.
34. Brütsch, R., Liebler, S.S., Wüstehube, J., Bartol, A., Herberich, S.E., Adam, M.G., Telzerow, A., Augustin, H.G. and Fischer, A. (2010) Integrin cytoplasmic domain-associated protein-1 attenuates sprouting angiogenesis. *Circ. Res.*, **107**, 592–601.
35. Voss, K., Stahl, S., Schleider, E., Ullrich, S., Nickel, J., Mueller, T.D. and Felbor, U. (2007) Evidence for anti-angiogenic and pro-survival functions of the cerebral cavernous malformation protein 3. *Neurogenetics*, **12**, 83–86.
36. Zhu, Y., Wu, Q., Xu, J.F., Miller, D., Sandalcioglu, I.E., Zhang, J.M. and Sure, U. (2010) Differential angiogenesis function of CCM2 and CCM3 in cerebral cavernous malformations. *Neurosurg. Focus*, **29**, E1.
37. McDonald, D.A., Shenkar, R., Shi, C., Stockton, R.A., Akers, A.L., Kucherlapati, M.H., Kucherlapati, R., Brainer, J., Ginsberg, M.H., Awad, I.A. *et al.* (2011) A novel mouse model of cerebral cavernous malformations based on the two-hit mutation hypothesis recapitulates the human disease. *Hum. Mol. Gen.*, **20**, 211–222.
38. Kuhn, R., Schwenk, F., Aguet, M. and Rajewsky, K. (1995) Inducible gene targeting in mice. *Science*, **269**, 1427–1429.